




Article

Effect of Process Parameters on the Generated Surface Roughness of Down-Facing Surfaces in Selective Laser Melting

Amal Charles ^{1,*} , Ahmed Elkaseer ^{1,2} , Lore Thijs ³, Veit Hagenmeyer ¹ and Steffen Scholz ^{1,4} 

¹ Institute for Automation and Applied Informatics, Karlsruhe Institute of Technology, 76344 Eggenstein-Leopoldshafen, Germany; ahmed.elkaseer@kit.edu (A.E.); veit.hagenmeyer@kit.edu (V.H.); steffen.scholz@kit.edu (S.S.)

² Faculty of Engineering, Port Said University, Port Fuad 42526, Egypt

³ Direct Metal Printing Engineering, 3D Systems, 3001 Leuven, Belgium; lore.thijs@3dsystems.com

⁴ Karlsruhe Nano Micro Facility, Hermann-von-Helmholtz-Platz 1, 76344 Eggenstein-Leopoldshafen, Germany

* Correspondence: amal.charles@kit.edu; Tel.: +49-721-608-25851

Received: 26 February 2019; Accepted: 20 March 2019; Published: 26 March 2019



Featured Application: This paper presents the first investigations towards closed loop feedback control of the selective laser melting (SLM) process. Insight gained from this work can be applied to facilitate in-process optimization of the SLM process for maximizing part quality and minimizing surface roughness.

Abstract: Additive manufacturing provides a number of benefits in terms of infinite freedom to design complex parts and reduced lead-times while globally reducing the size of supply chains as it brings all production processes under one roof. However, additive manufacturing (AM) lags far behind conventional manufacturing in terms of surface quality. This proves a hindrance for many companies considering investment in AM. The aim of this work is to investigate the effect of varying process parameters on the resultant roughness of the down-facing surfaces in selective laser melting (SLM). A systematic experimental study was carried out and the effects of the interaction of the different parameters and their effect on the surface roughness (S_a) were analyzed. It was found that the interaction and interdependency between parameters were of greatest significance to the obtainable surface roughness, though their effects vary greatly depending on the applied levels. This behavior was mainly attributed to the difference in energy absorbed by the powder. Predictive process models for optimization of process parameters for minimizing the obtained S_a in 45° and 35° down-facing surface, individually, were achieved with average error percentages of 5% and 6.3%, respectively, however further investigation is still warranted.

Keywords: additive manufacturing; selective laser melting; surface roughness; design of experiments; Ti6Al4V

1. Introduction

Since the advent of the first additive manufacturing (AM) technique, the Stereolithography process by 3D Systems in 1987, additive manufacturing has been under continuous and rapid development to meet growing industrial demands. Formerly, it was mainly used as a prototyping technique for pre-production, testing and analysis. However, different additive manufacturing techniques, which have recently emerged, play a significant role in modern industries [1,2].

This is principally because additive manufacturing has shown high potential to produce intricate 3D geometries with short lead-times at a relatively low cost. This helps strengthen supply chains and boosts their profitability and flexibility [3]. Presently, AM has been successfully exploited in electronic, aerospace and biomedical industries where highly specialized and customizable components are required [4–7]. The selective laser melting (SLM) technique makes especially great strides in the field of metal AM. This is especially achievable with the commercial emergence of titanium and nickel based super alloys that have exceptional material properties [7,8].

The SLM process is a powder bed additive manufacturing technique which uses a laser as a power source. The interaction between the laser and the metal powder causes the powder to selectively melt according to the desired slices. Once one layer is scanned, the platform is moved down by the height of this layer and another layer of powder is applied on top of the formerly built layer. This process of melting and bonding layers together continues successively until the desired part is built.

The non-melted powder remains in the build chamber and provides support to the part being built. This non-melted powder can be subsequently removed after building is completed and sieved; it can therefore be reused in successive builds [9].

Though noticeable progress has been made, there have been some challenging issues that still need addressing to allow AM and SLM to be used among mainstream manufacturing processes. Limited precision of the fabricated products and the repeatability of the processes are considered especially high technological barriers to the maturation of additive manufacturing techniques [4]. In particular, AM parts are often built with high surface roughness, which necessitates some post processing steps to refine the resultant roughness and makes it suitable for a wide range of engineering applications. These post-processing steps are rather expensive and time consuming.

The SLM process exhibits the so-called staircase effect in both up-facing and down-facing surfaces as depicted in Figure 1.

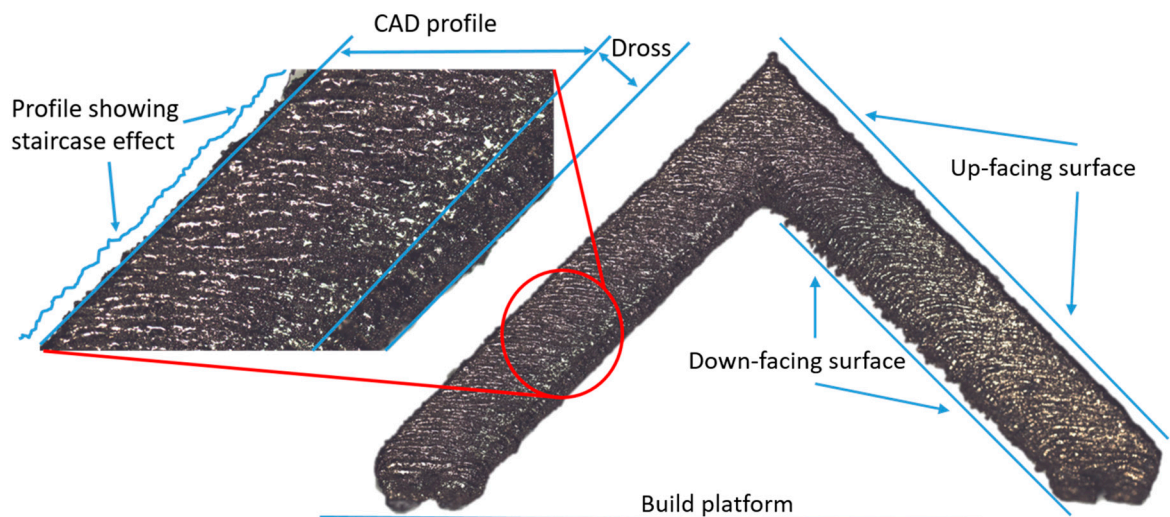


Figure 1. The staircase effect in up-facing and dross formation in down-facing surfaces in additive manufacturing (AM) parts.

This staircase effect contributes to the increased roughness of these surfaces. Down-facing surfaces, especially ones that are at an angle less than 45° , with respect to the build platform, show very high roughness. This is mainly attributed to the formation of dross and spatter due to the high laser absorptivity of powders compared to the solid metal in the bulk of the part as can be seen on Figure 2. The surface topology of parts produced by SLM are highly dependent on their orientation. This is why, in order to produce parts with good surface quality, down-facing surfaces with angles less than 45° are usually avoided by reorienting the part. Otherwise, there is a need for the building of support

structures. However, this in turn results in the increase of process steps, in particular, removal of the support could exhibit defects, such as burr formation, leading to even higher roughness [10].

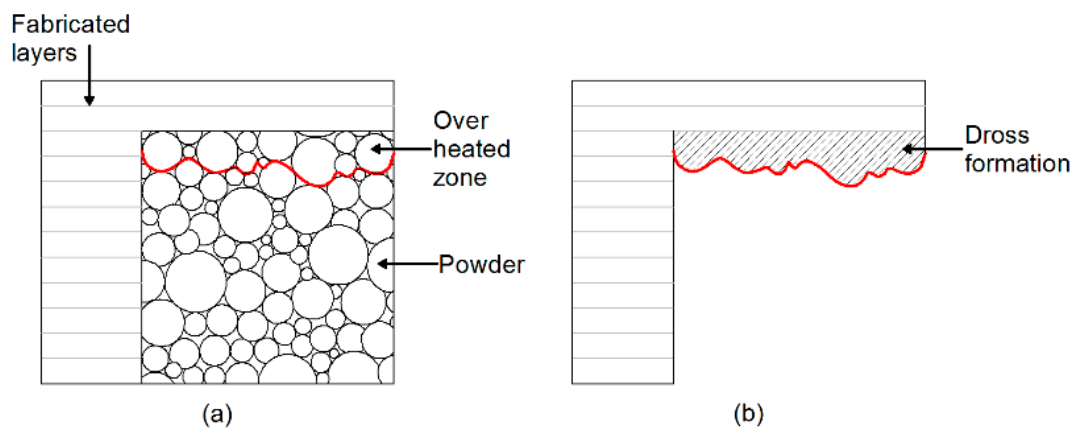


Figure 2. (a) A depiction of overheated zone above loose powder and (b) the resulting dross formation in the final part.

There have been some research attempts which try to correlate process parameters with quality marks of the parts, Sufiiarov et al. concluded that parts built with a 30 μm layer thickness demonstrated higher strength and lower elongations than parts built with a 50 μm layer thickness [11]. Wang et al. concluded that the mechanical properties of Inconel 718 parts did not vary along the build height of the parts [12].

Shipley et al. conducted a process optimization with the primary goal of maximizing part density, they identified the cooling rate to be important for the microstructural evolution and proposed methods to maintain a high energy input, which results in high cooling rates, thereby tailoring the microstructure and reducing residual stresses [13]. Evaluation of dimensional accuracy is a popular topic in AM research [14] as these technologies hold a lot of potential for application in research as well as industry. In this context, residual stresses are an important problem faced by the SLM process. These stresses can cause warping and deformation in parts thereby affecting the final dimensional accuracy and surface quality of printed parts. Therefore, many researchers have focused on the reduction of residual stresses and resulting substantial progress has been made in this field [15–17]. However, little research has been devoted to characterize the surface roughness of down-facing surfaces [18,19] and the optimization of parameters specifically for down-facing surfaces is, so far, an unexplored topic. In this context, the motivation for this work is to investigate and correlate the effects of different build parameters on the surface roughness of down-facing surfaces when the build parameters are only varied within the plane of the down-facing surface and its immediately adjacent volume as seen in Figure 3.

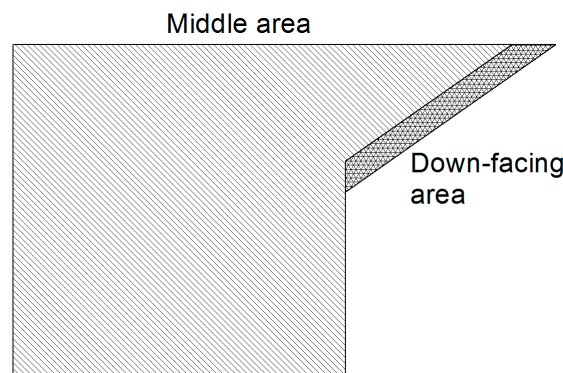


Figure 3. Illustration of areas printed with down-facing parameters.

2. Materials and Methods

2.1. Parameters

The parameters selected for this research work were laser power, scan speed and scan spacing. These were the parameters chosen as they are the ones considered most significant by a large body of research conducted in the metal AM field and have hence been the focus of many parameter optimization research works with regards to the SLM technique and powder bed AM techniques [20,21]. These parameters can easily be varied within the software of most printers and hence these are the parameters being considered in this work as well. It is to be noted that the parameters were varied only for the down-facing surfaces of the build as seen in Figure 3. The remainder of the part was built using the standard build parameters, as recommended by 3D Systems, for 60 μm layer thickness. The different levels of the parameter settings after rounding off can be seen in Table 1.

Table 1. Selected parameters and their levels.

Value	Laser Power	Scan Speed	Scan Spacing
−1	50	200	50
−0.59	90	465	60
0	150	850	75
0.59	210	1235	90
1	250	1500	100

2.2. Design of Experiments

Central composite method was used to design the experimental trials. This model was used as the limits for the factor settings. The design of experiments used to fabricate the test pieces can be seen in Table 2.

Table 2. Design of experiments.

Trial	Laser Power (W)	Scan Speed (mm/s)	Scan Spacing (μm)
1	90	465	60
2	90	465	90
3	90	1235	60
4	90	1235	90
5	210	465	60
6	210	465	90
7	210	1235	60
8	210	1235	90
9	50	850	75
10	250	850	75
11	150	200	75
12	150	1500	75
13	150	850	50
14	150	850	100
15	150	850	75
16	150	850	75
17	150	850	75
18	150	850	75
19	150	850	75
20	150	850	75
21	150	850	75
22	150	850	75
23	150	850	75
24	150	850	75

2.3. Test Piece

The test piece was designed to enable measure of the roughness of the down-facing surfaces. Consequently, the test pieces were designed to have a down-facing surface area of 10 mm × 20 mm and overhang inclinations of 45° and 35° as seen in Figure 4.

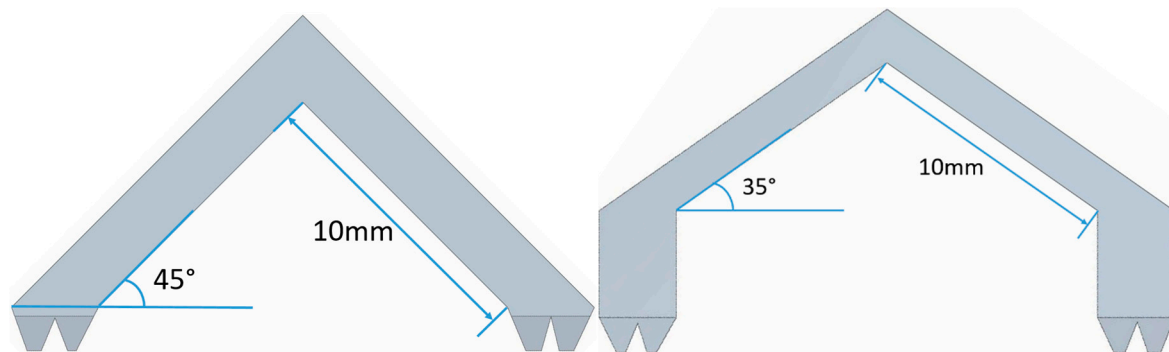


Figure 4. Depiction of CAD models with 45° and 35° overhangs.

2.4. Additive Manufacturing

The test pieces were designed using CAD Software Solid Edge (ST9, Siemens PLM software) and were directly imported into 3DXpert™ software (v13.0, 3D Systems) for the slicing, positioning and pre-processing of the build files. A 3D Systems ProX® DMP 320 machine (3D Systems, Leuven, Belgium) was used to perform the printing. The parts were heat treated before removal from the build platform in order to prevent warpage. The parts depicted in this paper were given a hexagonal cell scanning strategy and built with a 60 μm layer thickness. All parts were built using LaserForm Ti gr23 (A) powder.

2.5. Characterisation of Manufactured Parts

A Sensofar S neox 3D surface profiler (Sensofar, Barcelona, Spain) was used for the measurement of the surface roughness. The samples were subject to ultrasonic cleaning with water in order to detach any loose powder on the surface prior to measurement. A focus variation technique was used to scan the topography of a square of 4 mm × 4 mm dimension at the center of the down-facing surface for all samples. This scanned topography was then used to generate the areal roughness parameters.

3. Results and Statistical Analysis

A careful visual examination was conducted for all samples to characterize the visual appearance of the down-facing surfaces. Test pieces were visually examined to detect the presence of bright spots that could indicate spots of large spatter or dross presence, as shown in Figure 5.

Increased surface irregularities were observed in the 35° down-facing surface seen in Figure 5 (right) in the form of bright spots. This inferred the presence of spots of large spatter and dross formations. As can also be seen in the above image, this phenomenon was far less prominent in the 45° down-facing surface (left). This indicated a higher surface roughness in the 35° samples than the 45° samples. This indication was further confirmed by the experimental measurement results.

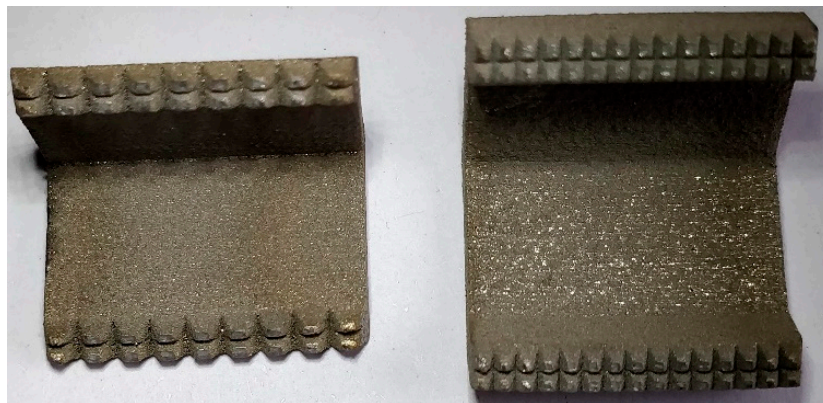


Figure 5. Visual observation of the down-facing surfaces shows significant irregularities of the surface in the 35° test piece (right) when compared to the 45° test piece (left).

3.1. Surface Roughness

The arithmetic mean height (S_a) parameter, which is an areal surface roughness parameter, expresses, as an absolute value, the difference in height of each point measured compared to the arithmetical mean of the surface. The S_a parameter has become one of the more popular methods for characterizing surface roughness of AM manufacturing parts because of the tendency of AM parts to have highly irregular and rough surfaces. Therefore, this parameter was chosen as the first quality mark for further process analysis.

The results presented herein in Figures 6 and 7 are for test pieces with an overhang angle of 45° and 35°, respectively.

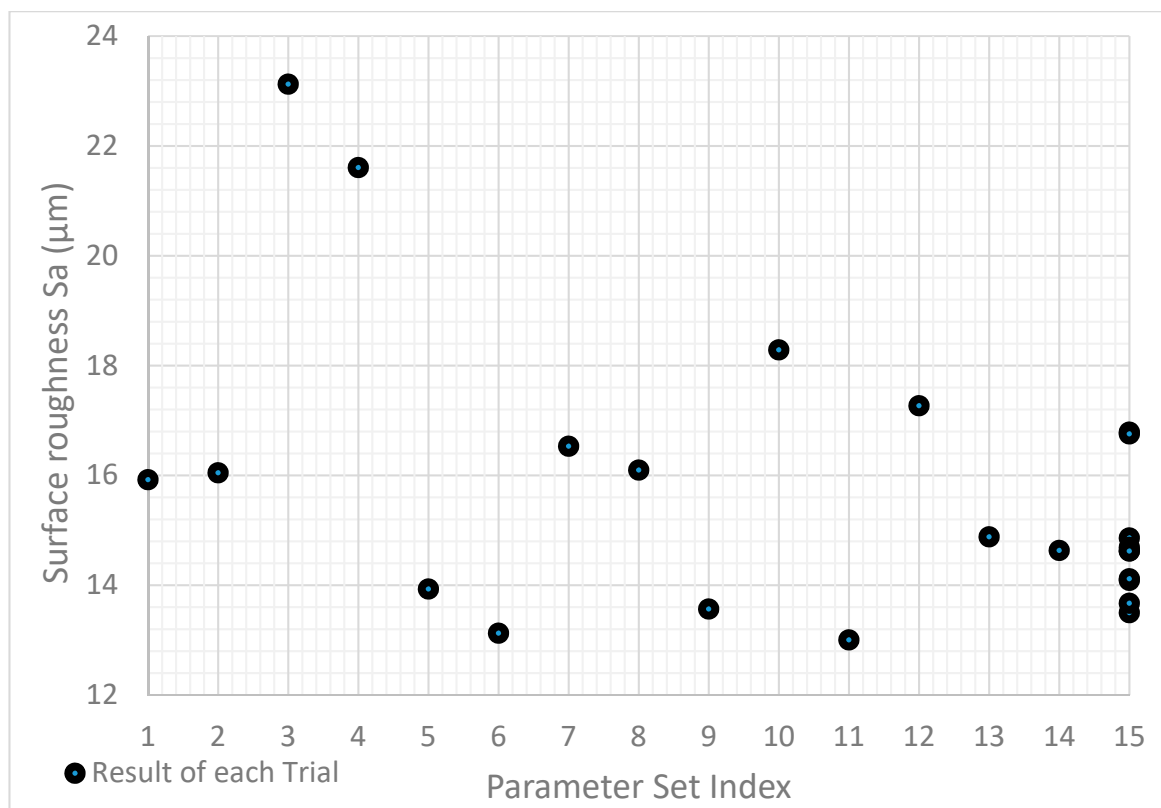


Figure 6. Replicate plot for 45° down-facing surfaces: Surface roughness (S_a) for each trial number.

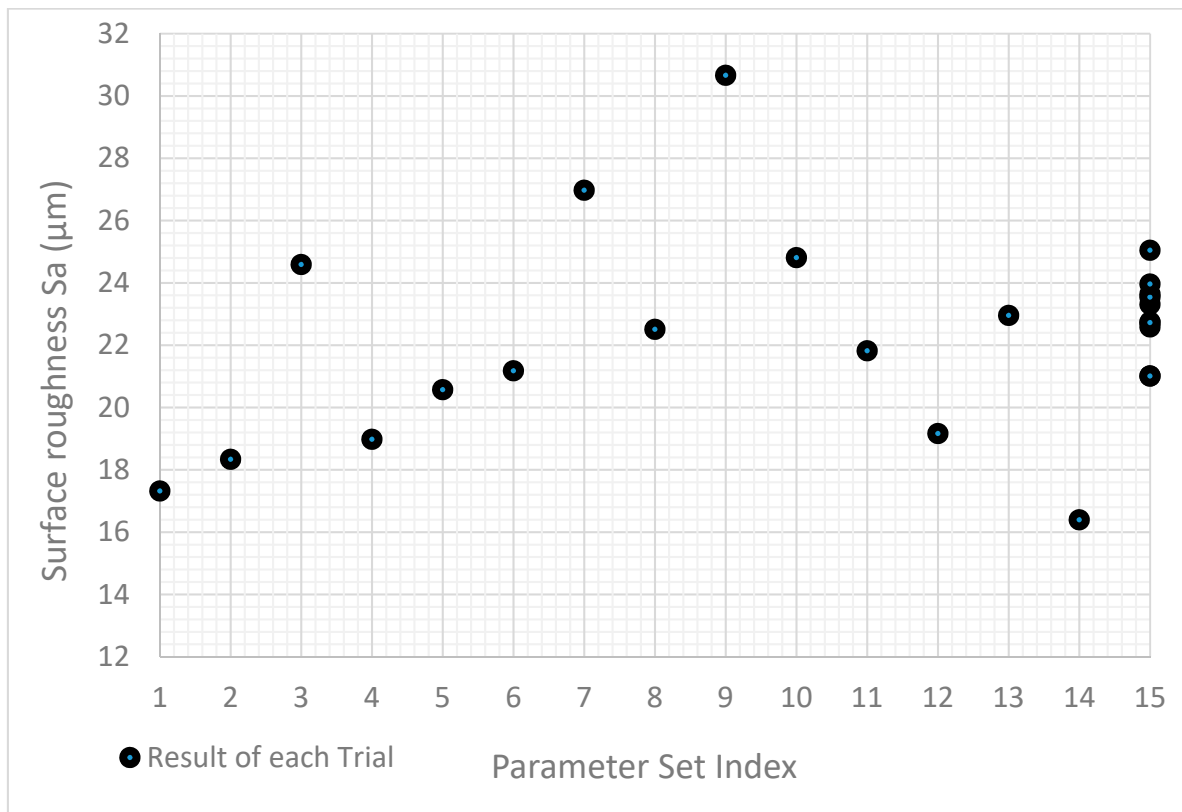


Figure 7. Replicate plot for 35° down-facing surfaces: Surface roughness (S_a) for each trial number.

The replicate plot shown in Figures 6 and 7 depicts the process as a stable process, thereby maximizing the possibility for developing a process model using these experimental results. By plotting the interaction effects of the various parameters on the obtained S_a as seen in Figures 8 and 9, clear trends can be seen thereby allowing us to draw conclusions.

3.2. Effect of Interaction of Parameters on S_a

3.2.1. Laser Power and Scan Speed

- 45° down-facing surface

Looking at the two graphs of laser power and scan speed in Figure 8, it is clear that for any given laser power, the S_a value increases with an increasing scan speed. The rate of increase in S_a varies at different laser powers. At lower laser powers, there is a rapid increase in S_a with increasing scan speed, while at higher laser powers the increase is only gradual.

The second graph depicts the decrease in S_a at different scan speeds when increasing the laser power up to a certain point, after which the S_a begins to gradually increase again. The laser power point at which the S_a begins to rise again varies amongst the different scan speeds.

- 35° down-facing surface

The 35° down-facing surfaces depict a different effect from the 45° surfaces. In this case, as seen in Figure 9 at the different laser powers, the S_a increases up to a scan speed of 1000 mm/s after which it begins to reduce once again.

3.2.2. Laser Power and Scan Spacing

- 45° down-facing surface

The interaction between laser power and scan spacing also shows clear trends. The S_a at the different laser powers gradually decreases when increasing scan spacing, however it tends to increase once it has passed the scan spacing of 80 μm .

The second graph shows that at all scan spacing levels, the S_a decreases up to a certain laser power (between 150 and 200 W) after which it begins to increase once again. While the laser power of 150 W showed the lowest S_a values.

- 35° down-facing surface

The effect of these parameters on the 35° down-facing surface also shows some difference when compared with the 45° down-facing surface, as seen in Figure 9. When increasing the scan spacing at different laser powers, the S_a values increase up to a scan spacing between 60 and 70 μm , after which they decrease. The laser power of 150 W showed the lowest S_a values.

3.2.3. Scan Speed and Scan Spacing

- 45° down-facing surface

It is quite clear from the first graph that at all scan spacings, the S_a value increases with an increase in scan speed. The second graph shows that at all the different scan speeds the S_a value will decrease up to a certain scan spacing value (80 μm) after which the S_a value increases once again. This is consistent with the observations made between laser power and scan spacing as well.

- 35° down-facing surface

In Figure 9, it can be seen that the effect of each scan spacing on the S_a shows an increase up to a certain scan speed, after which it begins to decrease once again. This point differs for each scan spacing, as can be seen in the graphs.

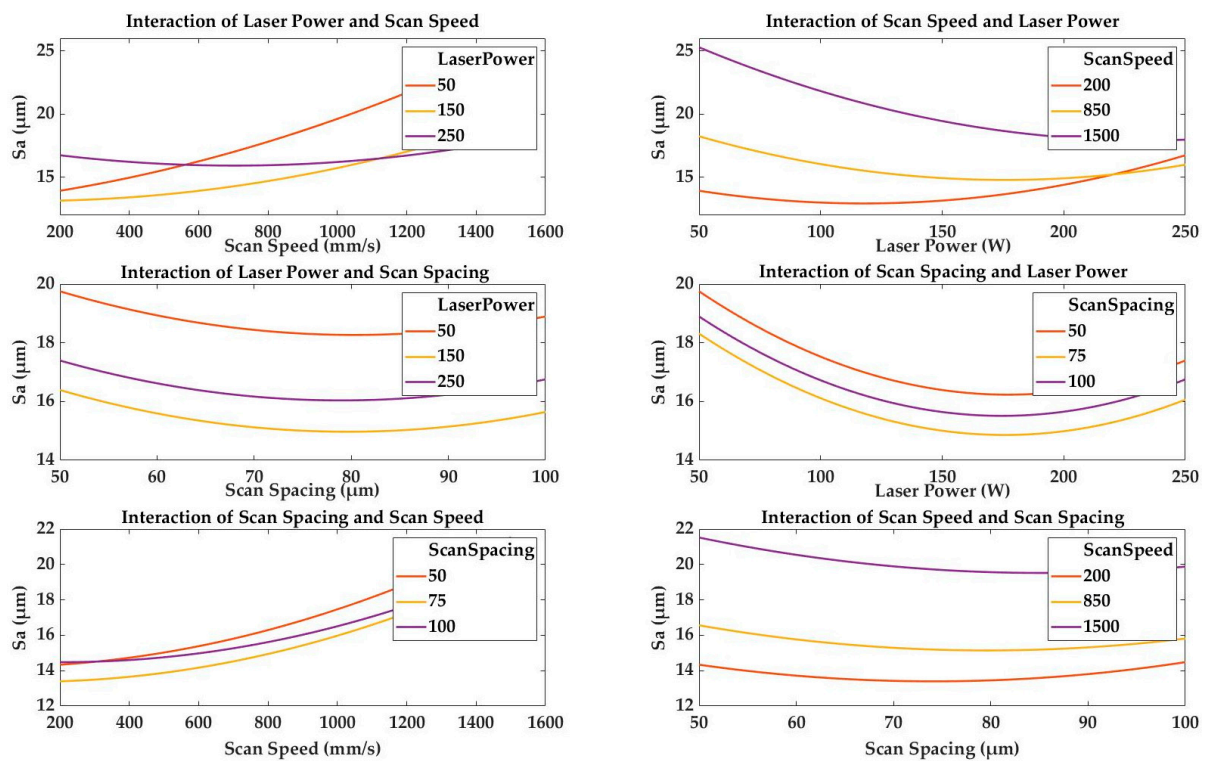


Figure 8. Interaction effects of parameters with the measured S_a for 45° down-facing surfaces.

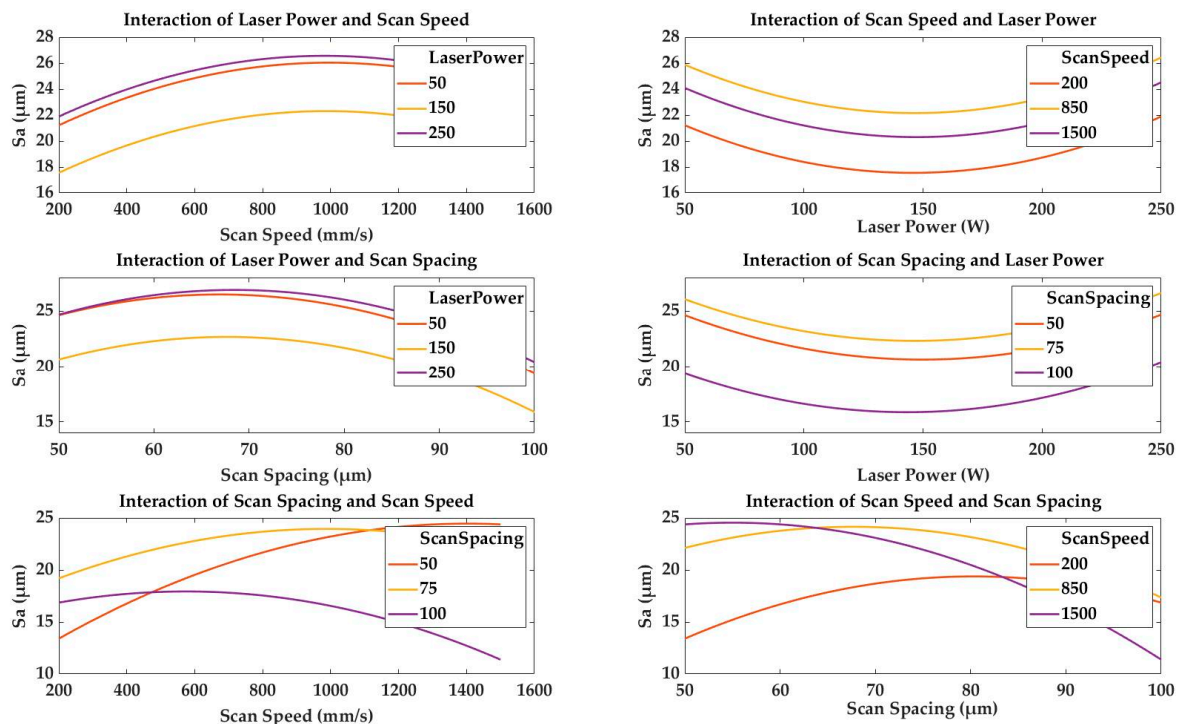


Figure 9. Interaction effects of parameters with the measured S_a for 35° down-facing surface.

The data processing and statistical modelling were completed using MATLAB (R2018b, MathWorks). A linear regression model with interaction effects was used to describe the relationship between parameters (laser power, scan speed and scan spacing) and S_a . The linear model was fit to the measured raw data, and this model was then used to generate the interaction plots as seen in Figures 8 and 9. These plots show the estimated effect on the response from changing each variable value, averaging out the effect of other parameters. This plot also shows the estimated effect when the other variable values are fixed at certain values as seen in Figures 8 and 9.

This same model also makes it possible to generate the prediction slice plots as seen in Figures 10 and 11. The prediction slice plots in Figures 10 and 11 show the main effects for all parameter values. The green line in each panel shows the change in the response variable as a function of the parameter values when all other predictor values are kept constant. The dashed red curves in each panel depict the 95% confidence bounds for the predicted response variable.

The plots shown in Figures 8 and 9 illustrate the effect of each predictor on the S_a model, with the objective being to minimize the obtainable surface roughness for the down-facing surface by understanding the effect of the down-facing parameters. It is now possible to use this predictive model in order to obtain parameters when minimizing the S_a . Obtaining a smoother surface by simply controlling the process parameters extends the current capabilities of printing inclined and down-facing surfaces without requiring the printing of support structures, thereby contributing to a reduction in post-processing times. To obtain an as-printed S_a of $12 \mu\text{m}$ would illustrate an improvement over current capabilities when printing with default parameters. Figure 9 suggests a set of parameters in order to achieve a S_a of $12.73 \mu\text{m}$, the corresponding normalized values for each process parameter were: Laser power = -0.35 (115 W), scan speed = -1 (465 mm/s) and scan spacing = -0.02 (approx. $75 \mu\text{m}$). For the 35° down-facing surface, a prediction of $20 \mu\text{m}$ would illustrate an improvement over current capabilities and with use of the developed model it was possible to predict process parameters to achieve this, as seen in Figure 11. The normalized value of parameters suggested were: Laser power = 0 (150 W), scan speed = 0.18164 (968 mm/s) and scan spacing = 0.56836 ($89 \mu\text{m}$). The predicted S_a and measured S_a values were determined to have an average error of 5% for 45° down-facing surfaces and 6.3% for 35° down-facing surfaces, which are

considered to be acceptable at this stage. However, further experiments and measurements are being conducted in order to further feed and develop the model.

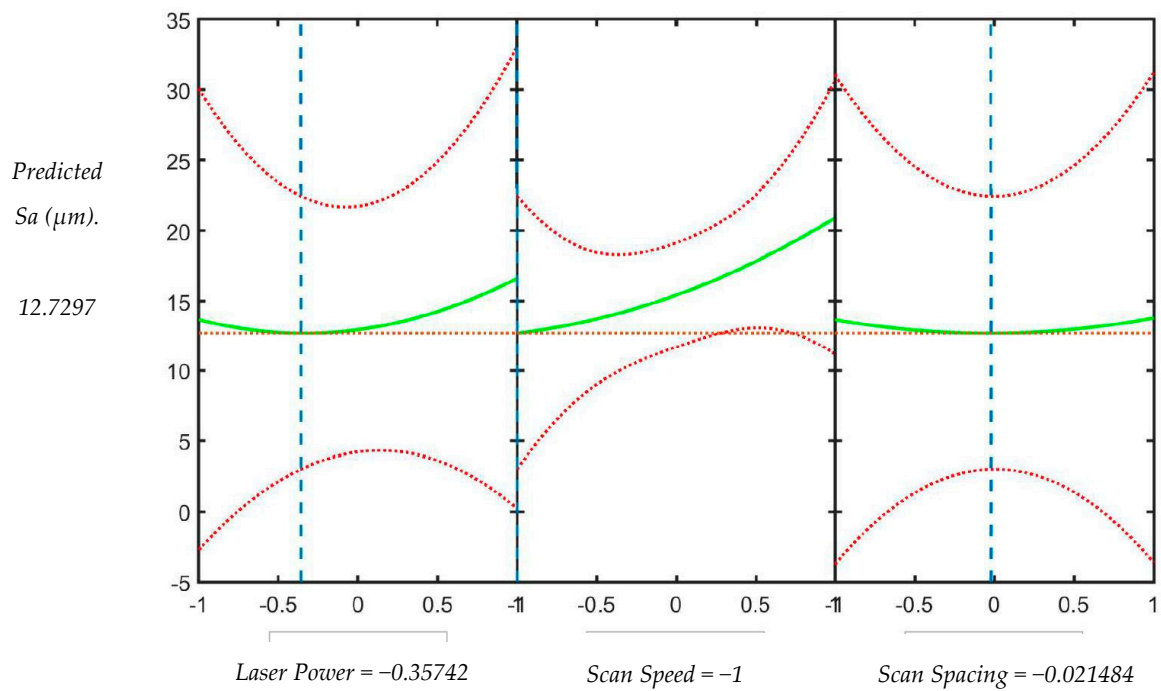


Figure 10. Effect of each parameter (normalized values) on the surface roughness model for down-facing surfaces.

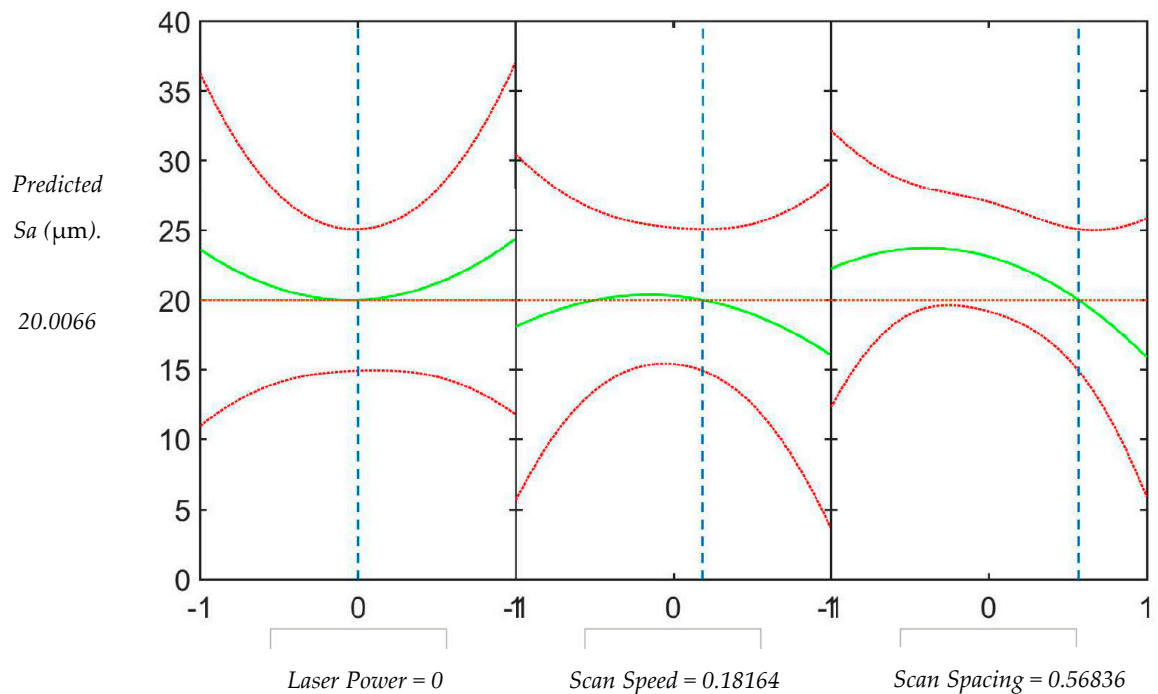


Figure 11. Effect of each parameter (normalized values) on the surface roughness model for a 35° down-facing surface.

4. Discussion

A close observation of Figure 12 confirms that one of the main reasons for the measured high S_a values for down-facing surfaces was unmelted or partially melted powder. The presence of

partially melted powder on the down-facing surface was almost unavoidable. This was caused during the printing process when the meltpool/dross that was formed came into contact with loose unsupported powder, thereby causing the partial melting of this loose powder and thereby the attachment/embedding of the loose powder within the surface of the desired printed part.

This aspect, coupled with the dross formation, which is formed by the full melting of loose powder in the overheated zones adjacent to the meltpool, were the major causes of high surface roughnesses in down-facing surfaces; this can be clearly seen in Figure 12.

Another observation made is that the 35° down-facing surfaces exhibited higher surface roughnesses than the 45° down-facing surfaces. It can be concluded that this occurred because, even though both surfaces were printed on top of loose powder, the 45° down-facing surface had a less steep slope when compared to the build platform, which resulted in a smaller overheating zone as some of the heat was conducted away through the solid bulk of the part. However, for the 35° down-facing surface a larger amount of energy was transferred into the powder, causing a larger meltpool and larger dross formation.

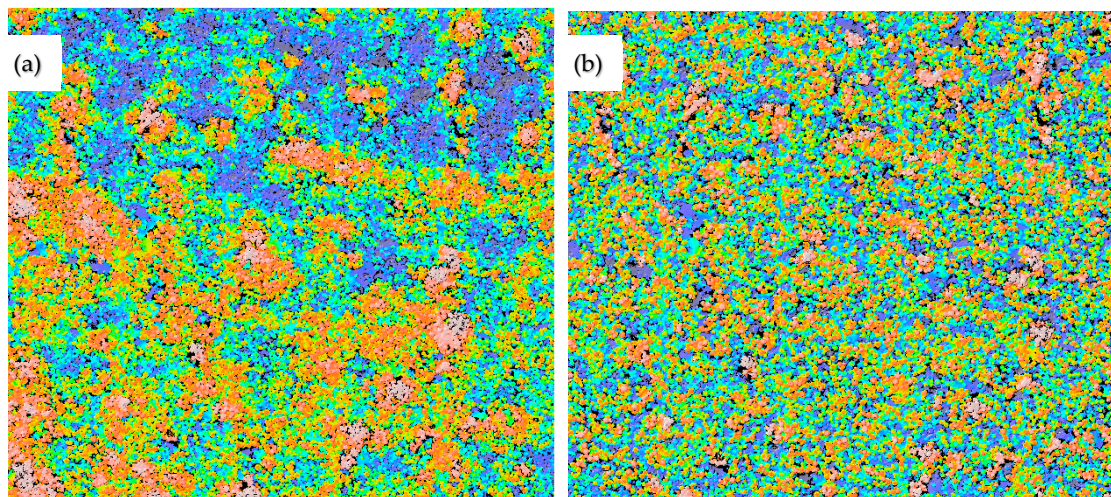


Figure 12. Microscopic images of the down-facing surfaces depicting the large presence of partially melted powder on the surface which thereby created surfaces with high roughness. (a) Unfiltered image, (b) image after filtering for waviness and roughness.

Additionally, while visually examining the samples it was found that some of the samples that showed relatively low surface roughness values in fact exhibited a significantly large dimensional deviation from the CAD of the samples. The down-facing surface was thicker than intended for many of the samples. This clearly indicated a large dross formation on the surface. This could be attributed to the larger energy input on some samples, resulting in the formation of larger meltpools. As a result, this could cause large dross with less measured roughness, as the larger meltpools had better wettability and would cause more interconnected melt pools which cause a uniform dross, and cannot be detected just by measuring roughness. Therefore, factors such as line energy, which could relate to the size of the meltpool formed, could lead to a better understanding of optimum overlap parameters in order to optimize the process for minimizing dross formation and surface roughness.

Dimensional accuracy tests are also required in order to investigate this phenomenon of formation of low roughness and large dross. It clearly becomes evident that, in the SLM process, the process parameters display significant degrees of interdependency that affects the final quality of printed parts.

5. Conclusions

This paper has presented a method to aid in the understanding of the effects of various SLM printing parameters on the surface roughness of down-facing surfaces. Clear trends were presented

on the interaction effects of the laser power, scan speed and scan spacing. Additionally, a predictive process model has also been presented for the suggestion of process parameters in order to attain a certain Sa value for 45° and 35° down-facing surfaces. Current works-in-progress are aimed at further improving this model by including more process data and also including other quality marks such as dimensional accuracy.

The experimental trials with the various parameter sets and replications showed that the process is stable and therefore made it possible to obtain a process model based on the three selected predictors and which uses Sa as the quality mark. This model was also used to optimize the process by suggesting process parameters with the objective of minimizing the Sa . The model was also tested by comparing the measured and predicted values; average errors of 5% (for 45° samples) and 6.3% (for 35° samples) were obtained. The continuous development of this model is currently taking place to include even more experimental data and quality marks. Process modelling by using artificial neural networks (ANN) is also an option and is being considered in order to further improve the process understanding and to minimize further the errors in prediction.

Such a model shows promise and is a step towards achieving a level of closed loop feedback control for the SLM process. By integrating it with existing pre-processing software, as well as other in-process monitoring tools, it will theoretically be able to assess the print quality during printing and make necessary changes as per the user's quality requirements. This system integration is planned for future work.

Author Contributions: Conceptualization, A.C., L.T., S.S.; methodology, A.C., A.E., L.T., S.S.; software, A.C., A.E.; validation, A.C., A.E., L.T.; formal analysis, A.C., A.E.; investigation, A.C., A.E.; resources, V.H., L.T., S.S.; data curation, A.C., A.E.; writing—original draft preparation, A.C.; writing—review and editing, A.C., A.E., L.T., V.H. and S.S.; visualization, A.C., A.E.; supervision, L.T., V.H. and S.S.; project administration, S.S.; funding acquisition, S.S.

Funding: This work was done in the H2020-MSCA-ITN-2016 project PAM², Precision Additive Metal Manufacturing, which is funded by The EU Framework Programme for Research and Innovation—Grant Agreement No. 721383.

Acknowledgments: The support by the Karlsruhe Nano Micro Facility (KNMF-LMP, <http://www.knmf.kit.edu/>) a Helmholtz research infrastructure at KIT, is gratefully acknowledged. The authors also acknowledge support by Deutsche Forschungsgemeinschaft and open access publishing fund of Karlsruhe Institute of Technology. The authors gratefully acknowledge the technical help provided by Fabian Grinschek from the Institute for Micro Process Engineering (IMVT) at Karlsruhe Institute of Technology, Germany.

Conflicts of Interest: The authors declare no conflict of interest.

References

1. Eyers, D.R.; Potter, A.T. Industrial Additive Manufacturing: A manufacturing systems perspective. *Comput. Ind.* **2017**, *92*, 208–218. [[CrossRef](#)]
2. Berman, B. 3-D printing: The new industrial revolution. *Bus. Horiz.* **2012**, *55*, 155–162. [[CrossRef](#)]
3. Brans, K. 3D Printing, A Maturing Technology. *IFAC Proc.* **2013**, *46*, 468–472. [[CrossRef](#)]
4. Kannan, G.B.; Rajendran, D.K. A Review on Status of Research in Metal Additive Manufacturing. In *Advances in 3D Printing & Additive Manufacturing Technologies*; Wimpenny, D.I., Pandey, P.M., Kumar, L.J., Eds.; Springer: Berlin/Heidelberg, Germany, 2017; pp. 95–100.
5. Clare, A.T.; Chalker, P.; Davies, S.; Sutcliffe, C.; Tsopanos, S. Selective laser melting of high aspect ratio 3D nickel–titanium structures two way trained for MEMS applications. *Int. J. Mech. Mater.* **2008**, *4*, 2. [[CrossRef](#)]
6. Rochus, P.; Plessier, J.Y.; Van Elsen, M.; Kruth, J.P.; Carrus, R.; Dormal, T. New applications of rapid prototyping and rapid manufacturing (RP/RM) technologies for space instrumentation. *Acta Astronaut.* **2007**, *61*, 1–6. [[CrossRef](#)]
7. Guo, N.; Leu, M.C. Additive manufacturing: Technology, applications and research needs. *Front. Mech. Eng.* **2013**, *8*, 215–243. [[CrossRef](#)]
8. Bourell, D.; Kruth, J.P.; Leu, M.; Levy, G.; Rosen, D.; Beese, A.M.; Clare, A.T. Materials for additive manufacturing. *CIRP Ann. Manuf. Technol.* **2017**, *66*, 659–681. [[CrossRef](#)]

9. Thijs, L.; Verhaeghe, F.; Craeghs, T.; Humbeeck, J.V.; Kruth, J.P. A study of the microstructural evaluation during selective laser melting of Ti-6Al-4V. *Acta Mater.* **2010**, *58*, 3303–3312. [[CrossRef](#)]
10. Triantaphyllou, A.; Giusca, C.L.; Macaulay, G.D.; Roerig, F.; Hoebel, M.; Leach, R.K.; Tomita, B.; Milne, K.A. Surface texture measurement for additive manufacturing. *Surf. Topogr. Metrol. Prop.* **2015**, *3*, 024002. [[CrossRef](#)]
11. Sufiiarov, V.S.; Popovich, A.A.; Borisov, E.V.; Polozov, I.A.; Masaylo, D.V.; Orlov, A.V. The Effect of Layer Thickness at Selective Laser Melting. *Procedia Eng.* **2017**, *174*, 126–134. [[CrossRef](#)]
12. Wang, X.; Keya, T.; Chou, K. Build Height Effect on the Inconel 718 Parts Fabricated by Selective Laser Melting. *Procedia Manuf.* **2016**, *5*, 1006–1017. [[CrossRef](#)]
13. Shipley, H.; McDonnell, D.; Culleton, M.; Coull, R.; Lupoi, R.; O'Donnell, G.; Trimble, D. Optimisation of process parameters to address fundamental challenges during selective laser melting of Ti-6Al-4V: A review. *Int. J. Mach. Tools Manuf.* **2018**, *128*, 1–20. [[CrossRef](#)]
14. Elkaseer, A.; Mueller, T.; Charles, A.; Scholz, S. Digital Detection and Correction of Errors in As-built Parts: A Step Towards Automated Quality Control of Additive Manufacturing. In Proceedings of the World Congress on Micro and Nano Manufacturing (WCMNM), Portorož, Slovenia, 18–20 September; pp. 389–392.
15. Tian, Y.; Tomus, D.; Rometsch, P.; Wu, X. Influences of processing parameters on surface roughness of Hastelloy X produced by selective laser melting. *Addit. Manuf.* **2017**, *13*, 103–112. [[CrossRef](#)]
16. Robinson, J.; Ashton, I.; Fox, P.; Jones, E.; Sutcliffe, C. Determination of the effect of scan strategy on residual stress in laser powder bed fusion additive manufacturing. *Addit. Manuf.* **2018**, *23*, 13–24. [[CrossRef](#)]
17. Kruth, J.-P.; Deckers, J.; Yasa, E.; Wauthlé, R. Assessing and comparing influencing factors of residual stresses in selective laser melting using a novel analysis method. *Proc. Inst. Mech. Eng. Part B J. Eng. Manuf.* **2012**, *226*, 980–991. [[CrossRef](#)]
18. Fox, J.C.; Moylan, S.P.; Lane, B.M. Effect of process parameters on the surface roughness of overhanging structures in laser powder bed fusion additive manufacturing. *Procedia CIRP* **2016**, *45* (Suppl. C), 131–134. [[CrossRef](#)]
19. Charles, A.; Elkaseer, A.; Mueller, T.; Thijs, L.; Torge, M.; Hagenmeyer, V.; Scholz, S. A Study of the Factors Influencing Generated Surface Roughness of Downfacing Surfaces in Selective Laser Melting. In Proceedings of the World Congress on Micro and Nano Manufacturing (WCMNM), Portorož, Slovenia, 18–20 September; pp. 327–330.
20. Khorasani, A.; Gibson, I.; Awan, U.S.; Ghaderi, A. The effect of SLM process parameters on density, hardness, tensile strength and surface quality of Ti-6Al-4V. *Addit. Manuf.* **2019**, *25*, 176–186. [[CrossRef](#)]
21. Shi, X.; Ma, S.; Liu, C.; Wu, Q. Parameter optimization for Ti-47Al-2Cr-2Nb in selective laser melting based on geometric characteristics of single scan tracks. *Opt. Laser Technol.* **2017**, *90*, 71–79. [[CrossRef](#)]

